ACS OMEGA

http://pubs.acs.org/journal/acsodf

Article

Synthesis, Characterization, DNA Binding, Anticancer, and Molecular Docking Studies of Novel Imidazolium-Based Ionic Liquids with Fluorinated Phenylacetamide Tethers

Nadjet Rezki,* Fawzia Faleh Al-blewi, Salsabeel A. Al-Sodies, Asaad Khalid Alnuzha, Mouslim Messali, Imran Ali, and Mohamed Reda Aouad*

Cite This: *ACS Omega* 2020, 5, 4807−4815

Read Online

ACCESS | Metrics & More | Article Recommendations | Supporting Information

ABSTRACT: Newer imidazolium ionic liquid (IL) halides **4a−f** appending variety of fluorinated phenylacetamide side chains were designed and synthesized through quaternization of 1-methyl and/or 1,2-dimethylimidazole with appropriate 2-chloro-*N*-(fluorinatedphenyl)acetamides. The resulting ILs were converted to their respective ionic liquid analogues carrying fluorinated counteranions (PF_6^-, BF_4^-, and/or CF_3COO^-) **5a−r**. All newly synthesized ILs were fully characterized using several spectroscopic experiments such as ^1H, ^{13}C, ^{11}B, ^{19}F, ^{31}P NMR, and mass analysis. The synthesized ionic liquids were investigated for their DNA binding and anticancer activities. The obtained DNA binding constants ranged from 1.444×10^5 to 3.518×10^5, indicating a reasonably good binding affinity. The percentage of anticancer activities ranged from 48 to 59 with H-1229 cell line, showing quite good anticancer potential. The modeling studies indicated the interactions of the reported molecules with DNA *via* hydrogen bonds. These were in agreement with those of DNA binding and anticancer results. Briefly, the designed ionic liquids may be used as good anticancer candidates for treating human cancer.

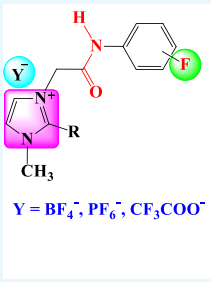

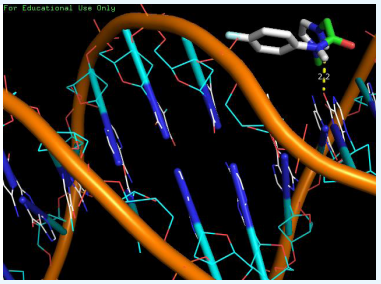

1. INTRODUCTION

The drug discovery is at the cutting edge of the most promising medicinal chemistry. The drug design is at a crossroad, facing growing strategies for the synthesis of new active pharmaceutical ingredients (APIs).[1] These strategies faced several challenges in the development of such scaffolds for effective drug delivery. These challenges are further exacerbated when drug compounds resulted from the combination of simple and active moieties with unique and tunable physicochemical and biological properties. Consequently, the development of potent anticancer agents is a major trend in drug discovery efforts in medicinal chemistry.[1,2] Ionic liquids (ILs) have been a topic of great interest in organic synthesis owing to their potential pharmaceutical properties and hold an important challenge in medicinal chemistry, especially in the race to synthesize new therapeutic agents or active pharmaceutical ingredients (APIs) tethered such moieties.[3] Generally, ILs are synthesized by combining organic cations such as imidazolium, pyridinium, ammonium, guanidinium, and phosphonium[4] with a wide variety of anions including halides (Cl^-, Br^-), hexafluorophosphate (PF_6^-), tetrafluoroborate (BF_4^-), trifluoroacetate (CF_3COO^-), bis-(trifluoromethylsulfonyl)amide (NTf_2), and dicyanamide (DCA).[5] These classes of ILs are well known as tunable molecules with unique physicochemical properties including low flammability, extremely low vapor pressure at room temperature, high ionic conductivity, and high thermal and chemical stabilities.[6] By modifying the cations and anions with special functional groups, all these properties may be adjustable with fascinating applications such as antiviral,[7] antibacterial,[8] antifungal,[9] anti-inflammatory,[10] and anticancer[11] activities.

In addition, several studies have been devoted to the use of ILs as antitumor agents against several human cancer cells such as breast,[12] brain,[13] colon,[14] lung,[15] liver,[16] osteosarcomas,[17] leukemia, and prostate.[18] In view of encouraging observations and as a continuation of our interest in the development of novel functionalized bioactive ionic liquids,[19−27] we have anticipated the synthesis of novel imidazolium-ionic liquids carrying fluorinated phenylacetamide. The synthesized ILs were tested with DNA binding and screened for their anticancer activities. Additionally, simulation studies were also investigated to determine the anticancer mechanism.

Received: October 17, 2019
Accepted: February 28, 2020
Published: March 9, 2020

Scheme 1. Synthesis of Ionic Liquids Bearing Imidazole Ring and Fluorinated Phenylacetamide Linkages 4a−f and 5a−r

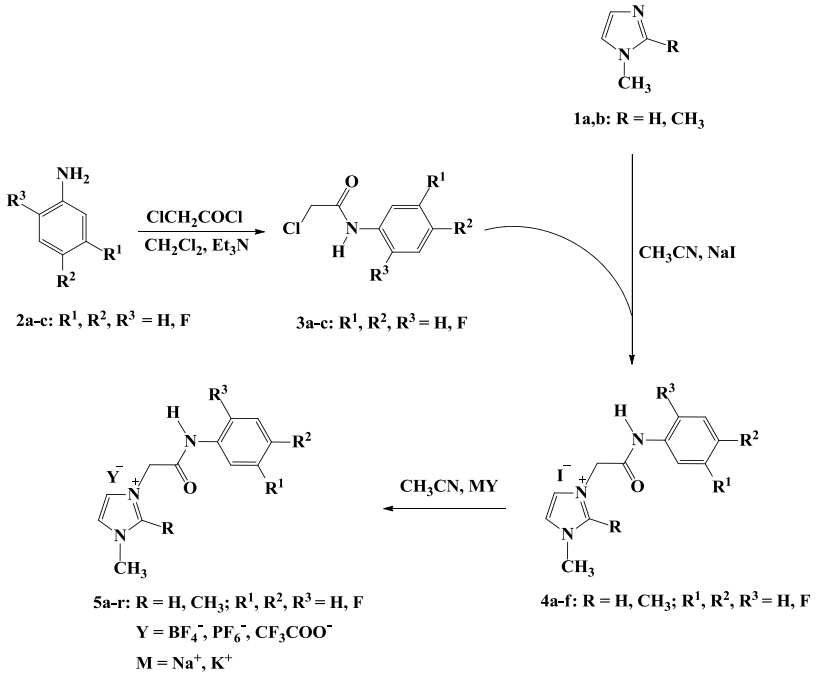

Table 1. Physical and Analytical Data for the Imidazolium IL Halides 4a−f

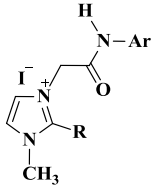

Comp. No	R	Ar	mp (°C)	Yield (%)	Comp. No	R	Ar	mp (°C)	Yield (%)
4a	H	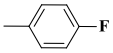	90-91 Colorless crystals	86	**4d**	CH_3		97-98 Colorless needles	87
4b	CH_3	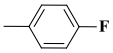	87-88 Colorless crystals	88	**4e**	H	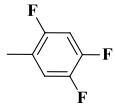	80-81 Colorless needles	90
4c	H		104-105 Colorless crystals	83	**4f**	CH_3	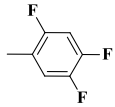	74-75 Colorless crystals	85

2. RESULTS AND DISCUSSION

2.1. Chemistry. A more holistic approach to design the desired imidazolium ionic liquids **4a−f** and **5a−r** is described in Scheme 1 and comprises quaternization and metathesis reactions.

Thus, the quaternization of sp^2 nitrogen atom of the substituted imidazoles **1** and/or **2** was carried out through their thermal alkylation by some aromatic acetamide chlorides **3a−c** for 2 h to afford the halogenated IL-based imidazolium−amide hybrids **4a−f** in 83−90% yields (Table 1).

It should be noted that the fluorinated phenyl acetamide precursors **3a−c** have been synthesized *via* base-assisted nucleophilic acylation of the appropriate fluorinated anilines with chloroacetyl chloride using triethylamine as a basic catalyst and dichloromethane as a solvent.

The structures of the resulted imidazolium iodides **4a−f** were elucidated based on their spectroscopic data. Their ^1H NMR spectra showed clearly the appearance of two distinct singlets at 4.64−5.29 and 10.39−10.77 ppm assigned to the NCH_2 and NHCO protons, which confirmed the success of the quaternization reaction. All the remaining protons were recorded in their respective area (see Experimental Section). In addition, the ^{13}C NMR spectra were in agreement with the designed structures. They exhibited new signals at 163.75−164.99 and 50.54−51.56 ppm belonging to the acetamide carbonyl (NHCO) and methylene (NCH_2) carbons, respectively.

https://dx.doi.org/10.1021/acsomega.9b03468
ACS Omega 2020, 5, 4807−4815

Table 2. Physical and Analytical Data of the Imidazolium ILs Carrying Fluorinated Counteranions 5a−r

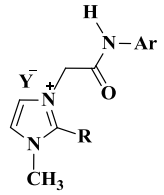

Comp. No	R	Ar	Y	mp (°C)	Yield (%)	Comp. No	R	Ar	Y	mp (°C)	Yield (%)
5a	H	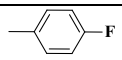	PF_6	75-76 Colorless crystals	87	**5j**	CH_3		PF_6	86-87 Light yellow crystals	88
5b	H	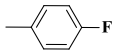	BF_4	Syrup	89	**5k**	CH_3		BF_4	Syrup	85
5c	H	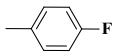	CF_3COO	66-67 Colorless crystals	90	**5l**	CH_3		CF_3COO	Syrup	83
5d	CH_3	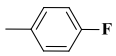	PF_6	69-70 Colorless needles	91	**5m**	H	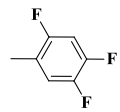	PF_6	Syrup	89
5e	CH_3	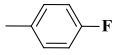	BF_4	Syrup	92	**5n**	H	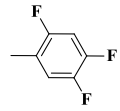	BF_4	Syrup	91
5f	CH_3	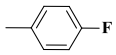	CF_3COO	Syrup	90	**5o**	H	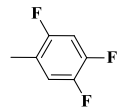	CF_3COO	Syrup	87
5g	H		PF_6	95-96 Colorless crystals	84	**5p**	CH_3	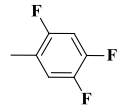	PF_6	Syrup	90
5h	H		BF_4	Syrup	87	**5q**	CH_3	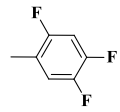	BF_4	Syrup	92
5i	H		CF_3COO	87-88 Colorless crystals	85	**5r**	CH_3	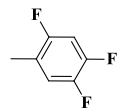	CF_3COO	Syrup	87

The resulting imidazolium iodides **4a−f** underwent a metathetical anion exchange *via* their treatment with appropriate fluorinated metal salts in acetonitrile furnishing on the elaboration of the desired task-specific imidazolium ionic liquids incorporating specific fluorinated anions (BF_4^-, PF_6^-, and CF_3COO^-) as counteranions **5a−r** (Scheme 1).

The structures of the obtained ILs **5a−r** were deduced from their spectroscopic data. It is noticeable that no changes were recorded on the signals that appeared in their ^1H and ^{13}C NMR spectra. This confirmed that the exchange occurred only on the counteranion. Thus, the presence of PF_6^- anion was evidenced by the ^{31}P and ^{19}F NMR spectra. The presence of a characteristic septet between −157.43 and −131.04 ppm in ^{31}P spectra, as well as a diagnostic doublet ranging from −69.18 to −69.16 ppm in their ^{19}F NMR spectra, supported the success of the PF_6^- anion exchange (Table 2).

On the other hand, the incorporation of tetrafluroborate (BF_4^-) anions on the specific imidazolium ionic liquids was evidenced based on their ^{31}B and ^{19}F NMR spectral data. Their ^{31}B NMR data showed a diagnostic multiplet near −1.32 to −1.29 ppm, but their ^{19}F NMR spectra exhibited two characteristic doublets around −148.23 to −148.14 ppm. However, the structures of the imidazolium ionic liquids, bearing the trifluoroacetate (CF_3COO^-) as a counter anion, were deduced based on their ^{19}F NMR spectra and showed a distinct singlet around −73.67 to −73.52 ppm attributed to such an anion. Additionally, all the spectra showed variable multiplets ranging from −141.60 to −118.31 ppm belonging to the aromatic fluorine atoms of the substituted phenyl rings (see Experimental Section).

2.2. DNA Binding Study. DNA is among the most significant pharmaceutical targets of anticancer medications.[28−30] Thus, studying the interactions of target compounds with DNA is important to get an indication about their anticancer impacts and imaginable mechanisms of action. In general, a compound and DNA formed covalent and noncovalent bonds. Through covalent bonding, a labile compound is switched by a nitrogen atom of the DNA base,

https://dx.doi.org/10.1021/acsomega.9b03468
ACS Omega 2020, 5, 4807−4815

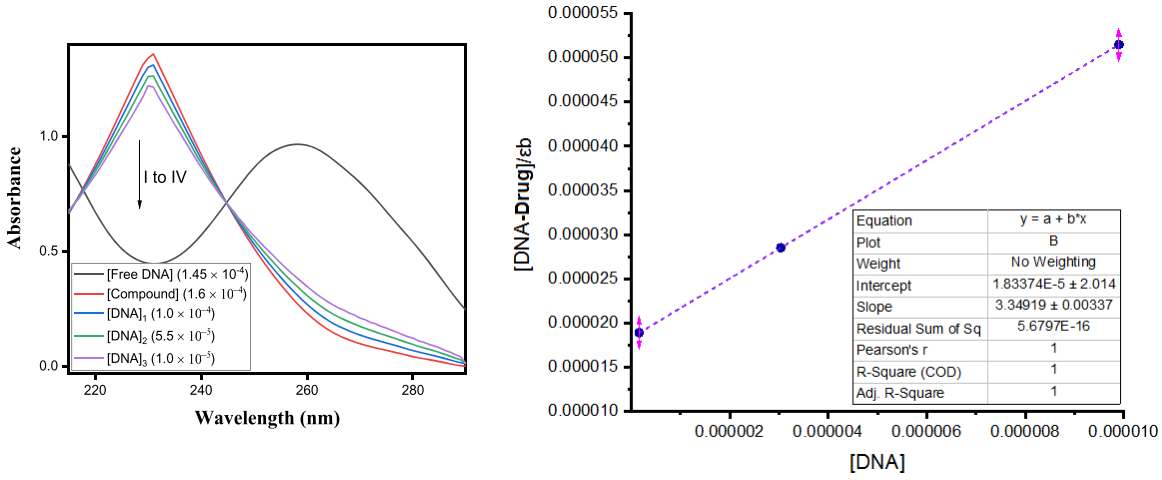

Figure 1. DNA binding study of compound **4a**.

such as N^7 of guanine, in which the interactions like electrostatic, intercalation, and groove binding are conceivable in non-covalent binding.[31] Meanwhile, The change in the wavelength or absorption or both is characteristic of the interactions and intercalative modes including strong stacking interactions between DNA base pairs and aromatic chromophores.[32] It is supposed that bathochromism means breakage of the secondary structure of DNA and hyperchromism involves covalent binding. Moreover, considerable red shifts revealed that the compounds were coordinated to DNA *via* N^7 position of guanine.[33] On the other hand, no or slight shifts in UV spectra are indicative of an outside groove binding, generally with minor hyperchromicity.[34]

In this study, the absorption bands of the tested ionic liquids **4a−f** and **5a−r** are recorded in the absence and presence of DNA. The spectra for **4a** are shown in Figure 1 as the representative one. The UV−vis spectral data for ILs **4a−f** and **5a−r** are summarized in Table 3. The DNA spectra for the remaining compounds are provided in the Supporting Information. Obviously, the absorption spectra of the compounds revealed the presence of absorption bands around 200 nm. The trivial shifts of the bands were assigned to 240−320 nm by adding DNA owing to the intraligand $\pi \rightarrow \pi^*$ and n $\rightarrow \pi^*$ transitions.[35,36] These minor shifts of the bands pointed to bathochromic shifts of all the compounds, which confirmed their interactions with DNA. Additionally, hypochromaticities were recorded for all the compounds with the addition of DNA in different concentrations (1.45×10^{-4} to 1.0×10^{-5} M). Such changes are obvious evidence of the formation of DNA adducts.[37] It is believed that these hypochromic shifts are probably due to the covalent and noncovalent bonds, which were observed in all target compounds.[38]

Furthermore, the values of DNA binding constants for all ILs range from 4.543×10^4 to 3.518×10^5, signifying a good interaction with DNA. The regression analysis was investigated by origin software for DNA binding readings. The resulted correlation coefficient (R^2) for each compound is also given in the respective figure and showed that almost all compounds interpolated through the minor groove with Ct-DNA. These results are bolstered by the accessible literature.[39] The literature referred that the compounds forming adducts with DNA through minor grooves and hydrophobic interactions as well as hydrogen bonds make major contribution adducts.[40,41] All these facts are well supported by the simulation studies.

Table 3. UV−Vis Data for Compounds 4a−f and 5a−r[a]

comp. no.	A_f	A_b	$\Delta\lambda_{max}$ (nm)	% hypochromism	K_b (M^{-1})
4a	1.311	1.123	0.188	14	1.825×10^5
4b	2.068	2.154	0.086	4	2.124×10^5
4c	1.594	1.422	0.172	10.7	2.547×10^5
4d	1.384	1.204	0.18	13	2.568×10^5
4e	0.553	0.503	0.05	9	1.5245×10^5
4f	0.029	0.025	0.004	13.7	2.356×10^5
5a	1.359	1.145	0.214	15.7	2.739×10^5
5b	0.13	0.113	0.017	13	1.832×10^5
5c	0.120	0.132	0.012	1	1.506×10^5
5d	0.218	0.226	0.008	3.6	1.444×10^5
5e	0.028	0.029	0.001	3.5	5.566×10^4
5f	2.350	2.261	0.089	3.7	1.693×10^5
5g	1.520	1.424	0.096	6	2.5×10^5
5h	1.745	1.549	0.196	11	1.928×10^5
5i	0.987	0.882	0.105	10	2.716×10^5
5j	0.023	0.026	0.003	13	2.40×10^5
5k	0.997	0.945	0.052	5	1.829×10^5
5l	1.265	1.153	0.112	8.8	1.935×10^5
5m	0.449	0.469	0.02	4	1.802×10^5
5n	0.591	0.523	0.068	11.5	4.543×10^4
5o	1.126	1.074	0.052	4.6	3.518×10^5
5p	0.145	0.150	0.005	3	2.303×10^5
5q	0.141	0.151	0.01	7	3.109×10^5
5r	1.549	1.305	0.244	15.7	3.032×10^5

[a]% Hypochromism (H%) = [change in λ_{max}/A_f] × 100, where A_f and A_b are the absorbances of free and bound compounds, respectively, K_b = binding constants, $\lambda_f = \lambda_{max}$ (free), $\lambda_b = \lambda_{max}$ (bound to DNA).

2.3. Anticancer Study. In vitro percentage inhibitions of lung cancer cell line H-1229 were used to assess the anticancer profiles of the tested ILs at 5.0, 10.0, 15.0, and 20.0 mM concentrations. The results are represented in Figure 2.

Initially, the tested molecules **4a−f**, **5a−5f**, **5-g−5l**, and/or **5m−5r** were dissolved in DMSO (0.1%), and natural cell by DMSO was used as vehicle control. The resulting mixtures were accumulated until the control cells touched an inactive phase. After 24 h, the cells were counted. The proliferation inhibitions were clearly enhanced with the increasing amount of compounds. The results exhibited a noteworthy inhibition in cancer cell proliferation. The maximum percentage of inhibitions were in the range of 48−59%. The inhibition ranges

https://dx.doi.org/10.1021/acsomega.9b03468
ACS Omega 2020, 5, 4807−4815

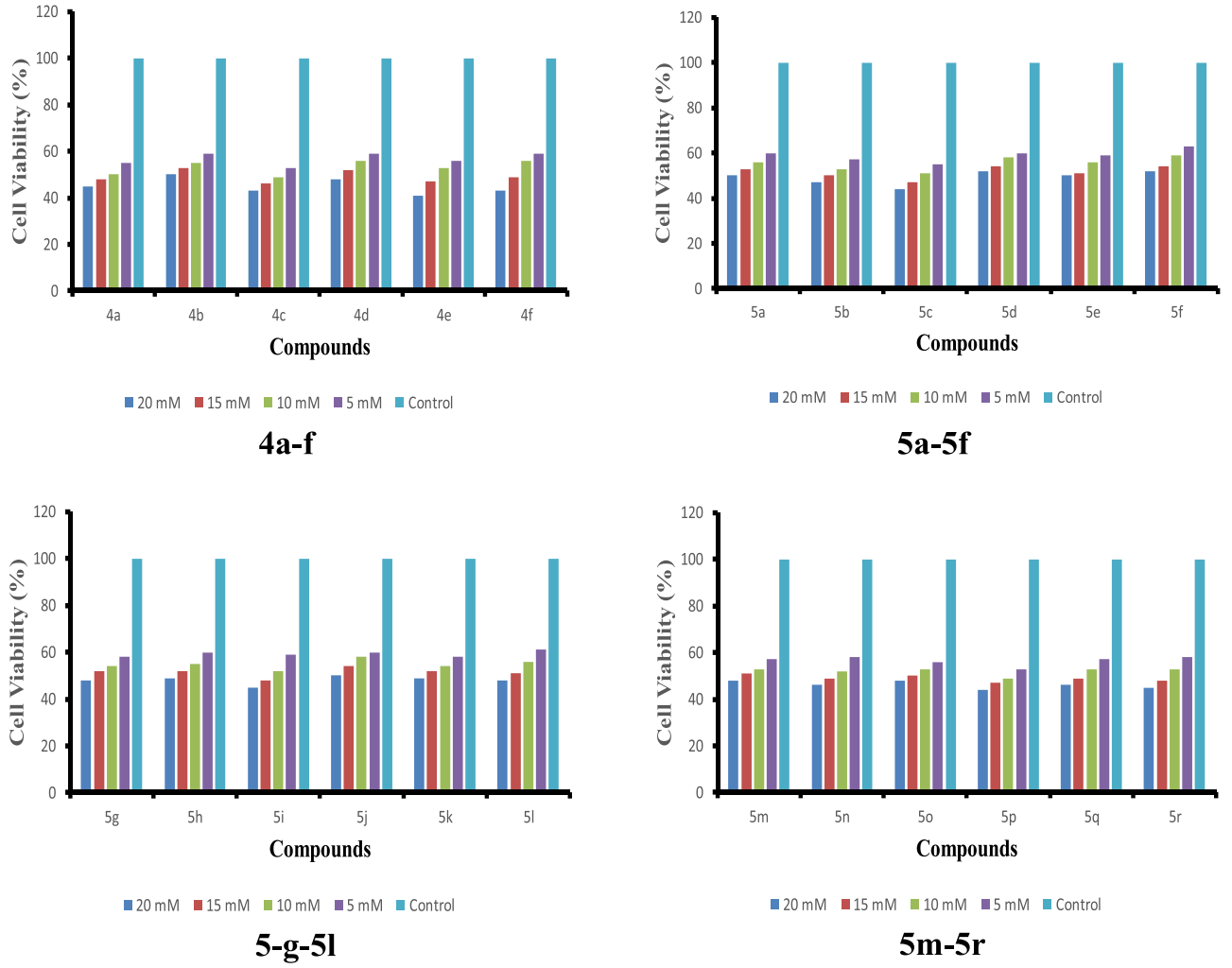

Figure 2. Anticancer profiles of the reported molecules with H-1229 cell line.

Table 4. Simulation Studies Results of the Reported Compounds with DNA

comp. no.	no. of H bonds	bond length (Å)	affinity in (kcal/mol)	hydrophobic interaction
4a	1	.263/A/DG′10/O6 & 'H' of −CONH- gp. (2.2)	−4.4	C1::dc15&dc9, C2::dc9, C3::dt8&dc9, C4::dc9, C5::O6, C8::dc15&dg14, C10::dg14&dc15, C12::O, N3::O6
4b	2	.263/A/DG′10/O6 & 'H' of −CONH- gp. (2.4)	−4.3	C2::dg14&O6, C4::dg14, C5::O6, C7::dc15, C8::dc15, C9::dc15, C10::dg14&dc15, C13::O6, N2::dc15, O::dc9
		.127/A/DC′9/N4 & 'O' of −CONH- gp. (3.4)		
4c	3	.263/A/DG′10/O6 & 'H' of −CONH- gp. (2.3)	−4.4	C2::dt8&dc9, C3::dc9, C5::O6, C6::dg14, C7::dg14, C8::dc15, C10::dc15, C12::dc15&O6, N2::dc15
		.263/A/DG′10/O6 & 'O' of −CONH- gp. (3.3)		
		.218/B/DG′14/N7 & 'O' of −CONH- (3.4)		
4d	1	.263/A/DG′10/O6 & 'H' of −CONH- gp. (2.5)	−3.9	C3::dc9, C4::dt8&dc9, C6::O6, C7::dg14, C8::dg14, C11::dc9&O6, C13::O6, N3::dg10&O6
4e	1	.263/A/DG′10/O6 & 'H' of −CONH- gp. (2.1)	−4.4	C1::dc9&dc15, C3::O6, C6::dg14&dc15, C8::dg14&dc15, C9::dc9&dt8, C10::dt8, C12::O6
4f	2	.263/A/DG′10/O6 & 'H' of −CONH- gp. (2.6)	−4.3	C1::dg14&O6, C4::O6, C5::dc15, C6::dc15, C7::dc15, C8::dc15&dg14, C10::dg14, C13::dc9&O6, N2::dc15
		.127/A/DC′9/N4 & 'O' of −CONH- gp. (3.4)		

of **4a−f**, **5a−5f**, **5-g−5l**, and **5m−5r** compounds were 50−59, 48−56, 50−55, and 52−56%, respectively. The percentage inhibitions were almost the same in all four series. The variations in the percentage inhibition were observed with the dissociation tendencies of the reported compounds. It was observed that highly dissociated molecules exhibited higher anticancer activities. This is probably because highly dissociate molecules provided a high concentration of positive ionic

https://dx.doi.org/10.1021/acsomega.9b03468
ACS Omega 2020, 5, 4807−4815

liquid parts to the DNA, leading to the higher binding with DNA and hence more activity. In the same manner, it was observed that bulky molecules showed low anticancer activities due to the steric effect. Thus, large-size molecules might have restricted their interactions with DNA. Overall, the total percentage inhibitions of 48−59% are quite good, and the reported molecules may be considered as potential anticancer agents for lung cancer.

2.4. Docking Study. It is important to mention here that out of 24 compounds, the basic organic moieties are 6 in **4a−f**. It is very clear that DNA docking study is carried out with organic moieties. Therefore, the docking study was carried out with six moieties of **4a−f** molecules. The obtained binding energies of the reported imidazolium ILs with DNA are summarized in Table 4 and were in the range from −3.9 to −4.4 kcal/mol. It is noticeable that the binding energies were variable due to the structure variation of the tested imidazolium compounds. Also, these structural differences also caused variation in hydrogen bond formation with DNA. Hydrogen bondings were found responsible for six moieties with DNA binding one hydrogen bond was formed between DNA and compounds **4a**, **4d**, and **4e**, while two hydrogen bonds were formed between DNA and compound **4b**. However, three hydrogen bonds were formed between DNA and compound **4c**. The hydrophobic interactions were also responsible for DNA interaction with the reported compounds. All the hydrophobic interactions with DNA are shown in Table 4. It was found that the DNA fragments involved with imidazolium were dc9, dc13, dc15, dg10, dg14, dc15, and dt8. The representative model of DNA binding with compound **4a** is shown in Figure 3, while the rest are given in the Supporting Information. On the contrary, the docked results clearly showed that all tested compounds reacted with DNA minor grooves. The docking model in Figure 3 clearly indicates DNA binding *via* DNA minor grooves. The DNA interaction process revealed that the orientation of all compounds was the same and such that their active sites were inside minor grooves. The DNA binding results were in agreement with the docking results.

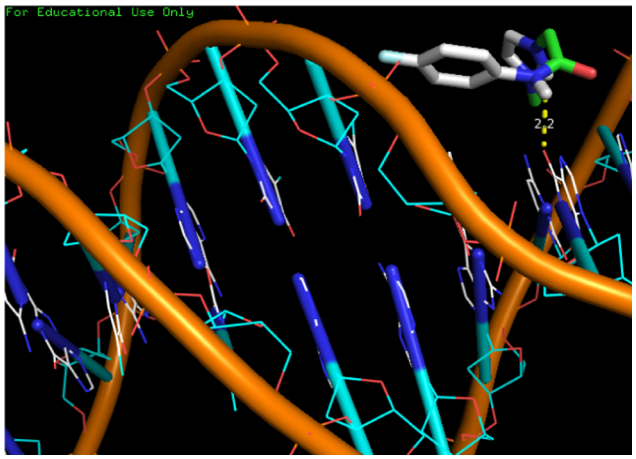

Figure 3. Docking model of compound **4a** with DNA.

3. CONCLUSIONS

Ionic liquids are gaining importance as anticancer molecules. Therefore, novel imidazolium ionic liquid halides tethering different fluorinated phenylacetamide side chains were prepared by quaternization of 1-methyl and/or 1,2-dimethylimidazole with appropriate 2-chloro-*N*-(fluorinatedphenyl)-acetamides. These were converted to their ionic liquid analogues having fluorinated counteranions (PF_6^-, BF_4^-, and/or CF_3COO^-). All newly synthesized ILs were characterized by various spectroscopic methods. The synthesized compounds were studied for DNA binding and anticancer activities with H-1229 cell line. Besides, the modeling studies were also carried out to investigate the DNA interaction mechanism of these molecules. The results of DNA binding, modeling, and anticancer activities indicated good interactions of these classes of compounds with DNA. Finally, it was concluded that these ionic liquids may be used as excellent anticancer candidates for treating human cancer.

4. EXPERIMENTAL SECTION

4.1. General Methods. Melting points were measured with a Stuart Scientific SMP1 apparatus and were uncorrected. All synthesized compounds were fully characterized by ^{1}H, ^{13}C, ^{19}F, ^{31}P, and ^{11}B NMR spectroscopy and HRMS. TLC was performed on aluminum plates silica gel (Kieselgel, 0.25 mm, 60 F254, Merck, Germany) and spots were visualized by ultraviolet (UV) light absorption using ethyl acetate/hexane as a developing solvent system. The NMR spectra were recorded with a 400 MHz Bruker NMR spectrometer. Chemical shifts (δ) were expressed in ppm using tetramethylsilane (TMS) as an internal standard. High-resolution mass spectroscopy (HRMS) was carried out using an LC-MS/MS impact II.

4.2. Synthesis and Characterization of 2-Chloro-*N*-(substituted phenyl)acetamides 3a−c. Chloroacetyl chloride (12 mmol) was added dropwise under stirring to a solution of appropriate fluorinated aniline **2a−c** (10 mmol) and triethylamine (12 mmol) in dichloromethane (40 mL) for 2 h at 0 °C. Then, the stirring was continued at room temperature for 6 h. The obtained precipitate was filtered, washed with water, and recrystallized from ethanol to afford the desired phenylacetamides **3a−c**.

*4.2.1. 2-Chloro-N-(4-fluorophenyl)acetamide (**3a**).* Colorless crystals, mp: 128−129 °C (lit. mp: 130 °C).[42] ^{1}H NMR (400 MHz, DMSO-d_6): δ_H = 4.34 (s, 2H, NC**H**$_2$), 7.55−7.60 (m, 2H, Ar-**H**), 7.79 (d, J = 8.0 Hz, 2H, Ar-**H**), 10.38 (s, 1H, CON**H**). ^{13}C NMR (100 MHz, DMSO-d_6): δ_C = 43.82 (N**C**H$_2$), 116.25, 121.97, 124.51, 135.68, 147.26, 158.70 (Ar-**C**), 164.87 (**C**═O). ^{19}F NMR (377 MHz, DMSO-d_6): δ_F = −118.57 to −118.50 (m, 1F, Ar-**F**).

*4.2.2. 2-Chloro-N-(2-fluorophenyl)acetamide (**3b**).* Colorless crystals, mp: 119−121 °C (lit. mp: 120−122 °C).[43] ^{1}H NMR (400 MHz, DMSO-d_6): δ_H = 4.41 (s, 2H, NC**H**$_2$), 7.21−7.30 (m, 3H, Ar-**H**), 7.82−7.90 (m, 1H, Ar-**H**), 10.24 (s, 1H, CON**H**). ^{13}C NMR (100 MHz, DMSO-d_6): δ_C = 43.5 (N**C**H$_2$), 116.36, 123.24, 125.23, 135.67, 146.32, 155.35 (Ar-**C**), 165.16 (**C**═O). ^{19}F NMR (377 MHz, DMSO-d_6): δ_F = −124.74 to −124.67 (m, 1F, Ar-**F**).

*4.2.3. 2-Chloro-N-(2,4,5-trifluorophenyl)acetamide (**3c**).* Colorless crystals, mp: 116−117 °C (lit. mp: 118−119 °C).[26] ^{1}H NMR (400 MHz, DMSO-d_6): δ_H = 4.34 (s, 2H, NC**H**$_2$), 7.66−7.70 (m, 1H, Ar-**H**), 7.94−8.02 (m, 1H, Ar-**H**), 10.30 (s, 1H, CON**H**). ^{13}C NMR (100 MHz, DMSO-d_6): δ_C = 43.46 (N**C**H$_2$), 106.65, 112.46, 123.12, 144.90, 147.08, 147.28, 150.67 (Ar-**C**), 165.85 (**C**═O). ^{19}F NMR (377 MHz, DMSO-d_6): δ_F = −141.76 to −141.62 (m, 1F, Ar-**F**), −139.11 to −139.04 (m, 1F, Ar-**F**), −125.60 to −125.51 (m, 1F, Ar-**F**).

https://dx.doi.org/10.1021/acsomega.9b03468
ACS Omega 2020, 5, 4807−4815

4.3. General Quaternization Procedure for the Synthesis of Imidazolium IL Halides 4a−f. 2-Chloro-*N*-(4-fluorophenyl)acetamide, 2-chloro-*N*-(4-fluorophenyl)-acetamide, and/or 2-chloro-*N*-(2,4,5-trifluorophenyl)-acetamide **3a−c** (10 mmol) were added with stirring to a solution of 1-methyl and/or 1,2-dimethyl imidazole **1a**,**b** (10 mmol) in acetonitrile (30 mL). Then, the mixture was refluxed for 2 h, until the completion of the reaction, as indicated by TLC (silicagel, hexane-ethyl acetate). The excess of the solvent was removed under reduced pressure. The obtained product was filtered and/or extracted by chloroform to yield the desired ionic liquids **4a−f**.

NB: Sodium iodide (10 mmol) was added during the synthesis of compounds **4a**, **4b**, **4e**, and **4f**.

The characterization of the imidazolium ILs **4a−f** is reported in the Supporting Information.

4.4. General Metathesis Procedure for the Synthesis of Imidazolium ILs Carrying Fluorinated Counteranions 5a−r. To a mixture of imidazolium IL halides **4a−f** (1 mmol) in acetonitrile (20 mL) was added suitable metal salts: potassium hexafluorophosphate, sodium tetrafluoroborate, and/or sodium trifluoroacetate (1.1 mmol) at room temperature under stirring. The reaction mixture was heated under reflux for 24 h. Then, the reaction mixture was cooled and filtered to eliminate solid metal halide. The acetonitrile was evaporated to afford quantitatively the desired imidazolium ionic liquids **5a−r**.

The characterization of the imidazolium ILs **5a−r** is reported in the Supporting Information.

4.5. DNA Binding Studies. The DNA binding experiments were carried out in Tris buffer (10^{-2} M, pH 7.2). Initially, the concentration of DNA was adjusted by recording the absorption spectrum of the CT-DNA solution. This solution showed UV absorbance at 230/260 nm (=1.8), indicating the free nature of DNA, with ε value equal to 6600 M^{-1} cm^{-1}.[44] The different solutions of the tested compounds and DNA were prepared and kept at 4 °C. First, the compounds were dissolved in DMSO (0.1%) and then diluted with Tris buffer till their concentrations became 2.4×10^{-4} M. Then, DNA was added in various concentrations ($1.2-1.5 \times 10^{-5}$ M) to record the respected absorption. Eventually, the binding constants (K_b) were calculated according to the Benessi−Hilderbrand eq 1.[45]

$$[DNA]/(\varepsilon_a - \varepsilon_f) = [DNA]/(\varepsilon_a - \varepsilon_f) + 1/K(\varepsilon_b - \varepsilon_f) \quad (1)$$

where absorption coefficients ε_a, ε_f, and ε_b are related to A_{obs}/[compound], extinction coefficient for the compounds in free as well in fully bound form. The binding constants (K_b) for different compounds were determined from slopes and the intercepts of the plots of

$$[DNA]/(\varepsilon_a - \varepsilon_f) \text{ vs } [DNA]$$

4.6. Anticancer Studies. The antiproliferative activity of the target imidazolium ILs was performed against lung cancer cell line H-1229 using the MTT assay. Thus, the cells were seeded (density of 8000 cells/well) in a 96-well plate and incubated. Around 60−70% confluency, the treatment of the cells with different concentrations of the reported compounds (5.0, 10.0, 15, and 20.0 mM) was carried out, followed by incubation for 24 h. The cells were assayed by adding 15.0 μL of 5.0 mg/mL MTT. Then, the respective media from each well were aspirated at 37 °C of incubation for 4 h. In 100 μL of DMSO, the cells were resuspended and the plate was instantly covered with aluminum foil and shook gently for 15 min. Absorbance was measured at 540 nm[46] and the percent inhibition of cellular proliferation was calculated using eq 2.

$$\% \text{ inhibitaion} = [A_{control} - A_{sample})/A_{control}] \times 100 \quad (2)$$

4.7. Docking Study. The docking readings were conducted using Windows XP operating system on Intel dual CPU (1.86 GHz). Marwin sketch was used in the drawing of the ligand 3D structure, which was transformed to the PDB file format. Ligand preparation was achieved by using AutoDock Tool (ADT) 4.0 version to allocate Gastegier charges, nonpolar hydrogens were merged, and then saved in PDBQT file format.[47] X-ray DNA crystal structure (PDB ID: 1bna) was retrieved from the Protein Data Bank (http://www.rcsb.org/pdb). The receptors were saved in the PDB file format using AutoDock Tools (ADT) 4.0, leaving heteroatoms (water). Besides, Gastegier charges were allocated to the receptor and then saved employing previous tools in the PDBQT file format. Preparation of parameter files for grid and docking was performed by means of ADT. Docking was carried out with AutoDock 4.0 (Scripps Research Institute) considering conformationally all the rotatable bonds of the ligand as rotatable and receptor as rigid.[41] Grid box size of 60 × 80 × 114 Å^3 with 0.375 Å spacing was used that encompassed the whole DNA. Macromolecule docking was done using an empirical-free energy function and Lamarckian genetic algorithm (LGA), with an initial population of 150 randomly placed individuals, a maximum number of 2 500 000 energy assessments, a crossover rate of 0.80, and a mutation rate of 0.02. For each ligand and serum−ligand adduct, at least 50 independent docking runs were performed for the lowest free energy of binding confirmation from the largest cluster and then saved in PDBQT format.

■ ASSOCIATED CONTENT

Supporting Information

The Supporting Information is available free of charge at https://pubs.acs.org/doi/10.1021/acsomega.9b03468.

Characterization of all newly synthesized compounds as well their respected NMR and mass spectra; DNA binding results and docking model of all newly synthesized compounds (PDF)

■ AUTHOR INFORMATION

Corresponding Authors

Nadjet Rezki − *Department of Chemistry, Faculty of Science, Taibah University, Al-Madinah Al-Munawarah 30002, Saudi Arabia; Department of Chemistry, Faculty of Sciences, University of Sciences and Technology Mohamed Boudiaf, Laboratoire de Chimie and Electrochimie des Complexes Metalliques (LCECM) USTO-MB, Oran 31000, Algeria*; Phone: +966537268682; Email: nadjetrezki@yahoo.fr

Mohamed Reda Aouad − *Department of Chemistry, Faculty of Science, Taibah University, Al-Madinah Al-Munawarah 30002, Saudi Arabia; Department of Chemistry, Faculty of Sciences, University of Sciences and Technology Mohamed Boudiaf, Laboratoire de Chimie and Electrochimie des Complexes Metalliques (LCECM) USTO-MB, Oran 31000, Algeria*; orcid.org/0000-0002-6876-4096; Phone: +966540953537; Email: mr_aouad@yahoo.fr

https://dx.doi.org/10.1021/acsomega.9b03468
ACS Omega 2020, 5, 4807−4815

Authors

Fawzia Faleh Al-blewi − *Department of Chemistry, Faculty of Science, Taibah University, Al-Madinah Al-Munawarah 30002, Saudi Arabia*

Salsabeel A. Al-Sodies − *Department of Chemistry, Faculty of Science, Taibah University, Al-Madinah Al-Munawarah 30002, Saudi Arabia*

Asaad Khalid Alnuzha − *Department of Chemistry, Faculty of Science, Taibah University, Al-Madinah Al-Munawarah 30002, Saudi Arabia*

Mouslim Messali − *Department of Chemistry, Faculty of Science, Taibah University, Al-Madinah Al-Munawarah 30002, Saudi Arabia*

Imran Ali − *Department of Chemistry, Faculty of Science, Taibah University, Al-Madinah Al-Munawarah 30002, Saudi Arabia; Department of Chemistry, Jamia Millia Islamia (A Central University), New Delhi 110025, India*

Complete contact information is available at: https://pubs.acs.org/10.1021/acsomega.9b03468

Author Contributions

All authors discussed the results and commented on the manuscript.

Notes

The authors declare no competing financial interest.

■ ACKNOWLEDGMENTS

The authors thank the Chemistry Department at Taibah University for providing the facilities in sample analysis.

■ REFERENCES

(1) Taylor, J. B.; Kennewell, P. D.; Horwood, E. Modern Medicinal Chemistry. *Trends Pharmacol. Sci.* **1994**, *15*, 350−351.

(2) Patil, S. A. A Role of Medicinal Chemist in the Modern Drug Discovery and Development. *Org. Chem.: Curr. Res.* **2012**, *1*, 1−2.

(3) (a) Ferraz, R.; Branco, L. C.; Prudêncio, C.; Noronha, J. P.; Petrovski, Ž. Ionic Liquids as Active Pharmaceutical Ingredients. *Chem. Med. Chem.* **2011**, *6*, 975−985. (b) Kellar, R.; Nieto, N. C.; Koppisch, A.; Del Sesto, R. Ionic liquids that sterilize and prevent biofilm formation in skin wound healing devices. U.S. Patent US20180093011A1, Sept 19, 2019.

(4) Marrucho, I. M.; Branco, L. C.; Rebelo, L. P. N. Ionic Liquids in Pharmaceutical Applications. *Annu. Rev. Chem. Biomol. Eng.* **2014**, *5*, 527−546.

(5) Balk, A.; Holzgrabe, U.; Meinel, L. 'Pro et contra' ionic liquid drugs-Challenges and opportunities for pharmaceutical translation. *Eur. J. Pharm. Biopharm.* **2015**, *94*, 291−304.

(6) (a) Egorova, K. S.; Gordeev, E. G.; Ananikov, V. P. Biological activity of ionic liquids and their application in pharmaceutics and medicine. *Chem. Rev.* **2017**, *117*, 7132−7189. (b) Shamshina, J. L.; Berton, P.; Wang, H.; Zhou, X.; Gurau, G.; Rogers, R. D. Ionic Liquids in Pharmaceutical Industry. In *Green Techniques for Organic Synthesis and Medicinal Chemistry*, 2nd ed.; Zhang, W.; Cue, B. W., Eds.; Wiley, 2018. (c) MacFarlane, D. R.; Kar, M.; Pringle, J. M. *Fundamentals of Ionic Liquids from Chemistry to Application*; Wiley-VCH, 2017. (d) McKee, M. A. Ionic liquids for agricultural residue removal. U.S. Patent US20140128626A1, May 8, 2014. (e) Qu, J.; Luo, H. Corrosion prevention of magnesium surfaces via surface conversion treatments using ionic liquids. U.S. Patent US20150090369A1, April 2, 2015. (f) Wu, B.; Holbrey, J. D.; Reddy, R. G.; Rogers, R. D. Ionic liquid temperature sensor. U.S. Patent US6749336B2, June 15, 2004.

(7) Kumar, V.; Malhotra, S. V. Synthesis of nucleoside-based antiviral drugs in ionic liquids. *Bioorg. Med. Chem. Lett.* **2008**, *18*, 5640−5642.

(8) Anvari, S.; Hajfarajollah, H.; Mokhtarani, B.; Enayati, M.; Sharifi, A.; Mirzaei, M. Antibacterial and Anti-Adhesive Properties of Ionic Liquids with Various Cationic and Anionic Heads toward Pathogenic Bacteria. *J. Mol. Liq.* **2016**, *221*, 685−690.

(9) Ranjan, P.; Kitawat, B. S.; Sing, M. 1-Butylimidazolederived ionic liquids: synthesis, characterisation and evaluation of their antibacterial, antifungal and anticancer activities. *RSC Adv.* **2014**, *4*, 53634−53644.

(10) Azevedo, A. M. O.; Costa, S. P. F.; Diasa, A. F. V.; Marquesa, A. H. O.; Pintoa, P. C. A. G.; Bicac, K.; Ressmannc, A. K.; Passosa, M. L. C.; Araújoa, A. R. T. S.; Reise, S.; Saraiva, M. L. M. F. S. Antiinflammatory choline based ionic liquids: Insights into their lipophilicity, solubility and toxicity parameters. *J. Mol. Liq.* **2017**, *232*, 20−26.

(11) Dias, A. R.; Costa-Rodrigues, J.; Fernandes, M. H.; Ferraz, R.; Prudêncio, C. Anti-cancer potential of Ionic Liquids. *Chem. Med. Chem.* **2017**, *12*, 11−18.

(12) Kumar, V.; Malhotra, S. V. Study on the potential anticancer activity of phosphonium and ammonium-based ionic liquids. *Bioorg. Med. Chem. Lett.* **2009**, *19*, 4643.

(13) Kaushik, N. K.; Attri, P.; Kaushik, N.; Choi, E. H. Synthesis and Antiproliferative Activity of Ammonium and Imidazolium Ionic Liquids against T98G Brain Cancer Cells. *Molecules* **2012**, *17*, 13727−13739.

(14) Frade, R. F. M.; Matias, A.; Branco, L. C.; Afonso, C. A. M.; Duarte, C. M. M. Effect of Ionic Liquids on Human Colon Carcinoma HT-29 and CaCo-2 Cell Lines. *Green Chem.* **2007**, *9*, 873−877.

(15) Chen, H.-L.; Kao, H.-F.; Wang, J.-Y.; Wei, G.-T. Cytotoxicity of Imidazole Ionic Liquids in Human Lung Carcinoma A549 Cell Line. *J. Chin. Chem. Soc.* **2014**, *61*, 763−769.

(16) Torrecilla, J. S.; García, J.; Rojo, E.; Rodríguez, F. Estimation of toxicity of ionic liquids in Leukemia Rat Cell Line and Acetylcholinesterase enzyme by principal component analysis, neural networks and multiple lineal regressions. *J. Hazard. Mater.* **2009**, *164*, 182−194.

(17) Ferraz, R.; Costa-Rodrigues, J.; Fernandes, M. H.; Santos, M. M.; Marrucho, I. M.; Rebelo, L. P. N.; Prudêncio, C.; Noronha, J. P.; Petrovski, Z.; Branco, L. C. Antitumor Activity of Ionic Liquids Based on Ampicillin. *Chem. Med. Chem.* **2015**, *10*, 1480−1483.

(18) Bubalo, M. C.; Radošević, K.; Srček, V. G.; Das, R. N.; Popelier, P.; Roy, K. Cytotoxicity towards CCO Cells of Imidazolium Ionic Liquids with Functionalized Side Chains: Preliminary QSTR Modeling Using Regression and Classification Based Approaches. *Ecotoxicol. Environ. Saf.* **2015**, *112*, 22−28.

(19) Rezki, N.; Al-Sodies, S. A.; Aouad, M. R.; Bardaweel, S.; Messali, M.; El Ashry, E. H. An eco-friendly ultrasound-assisted synthesis of novel fluorinated pyridinium salts-based hydrazones and antimicrobial and antitumor screening. *Int. J. Mol. Sci.* **2016**, *17*, 766−785.

(20) Rezki, N.; Al-Sodies, S. A.; Shreaz, S.; Shiekh, R. A.; Messali, M.; Raja, V.; Aouad, M. R. Green ultrasound versus conventional synthesis and characterization of specific task pyridinium ionic liquid hydrazones tethering fluorinated counter anions: Novel inhibitors of fungal Ergosterol biosynthesis. *Molecules* **2017**, *22*, 1532−1552.

(21) Aljuhani, A.; El-Sayed, W. S.; Sahu, P. K.; Rezki, N.; Aouad, M. R.; Salghi, R.; Messali, M. Microwave-assisted synthesis of novel imidazolium, pyridinium and pyridazinium-based ionic liquids and/or salts and prediction of physico-chemical properties for their toxicity and antibacterial activity. *J. Mol. Liq.* **2018**, *249*, 747−753.

(22) Rezki, N.; Messali, M.; Al-Sodies, S. A.; Naqvi, A.; Bardaweel, S. K.; Al-blewi, F. F.; Aouad, M. R.; El Ashry, E. H. Design, Synthesis, *in-silico* molecular docking and evaluation of di-cationic pyridinium ionic liquids as potential anticancer scaffolds. *J. Mol. Liq.* **2018**, *265*, 428−441.

(23) Rezki, N.; Al-Sodies, S. A.; Messali, M.; Bardaweel, S. K.; Sahu, P. K.; Al-blewi, F. F.; Sahu, P. K.; Aouad, M. R. Identification of new pyridinium ionic liquids tagged Schiff base: Design, synthesis, *in silico* ADMET prediction and biological evaluation. *J. Mol. Liq.* **2018**, *264*, 367−374.

(24) Albalawi, A. H.; El-Sayed, W. S.; Aljuhani, A.; Almutairi, S. M.; Rezki, N.; Aouad, M. R.; Messali, M. Microwave assisted synthesis of some potential bioactive imidazolium-based room temperature ionic liquids. *Molecules* **2018**, *23*, 1727−1741.
(25) Al-Blewi, F. F.; Rezki, N.; Al-Sodies, S. A.; Bardaweel, S. K.; Sabbah, D. A.; Messali, M.; Aouad, M. R. Novel cationic amphiphilic fluorinated pyridinium hydrazones: conventional versus green ultrasound assisted synthesis, characterization, molecular docking, and anticancer evaluation. *Chem. Cent. J.* **2018**, *12*, No. 118.
(26) Aljuhani, A.; Aouad, M. R.; Rezki, N.; Aljaldy, O. A.; Al-Sodies, S. A.; Messali, M.; Ali, I. Novel pyridinium based ionic liquids with amide tethers: Microwave assisted synthesis, molecular docking and anticancer studies. *J. Mol. Liq.* **2019**, *285*, 790−802.
(27) Al-blewi, F. F.; Rezki, N.; Bardaweel, S. K.; Naqvi, A.; Qutb eddn, H. A. B.; Al-Sodies, S. A.; Messali, M.; Aouad, M. R. A profile of the *in vitro* anti-tumor activity against breast and colon cancer cell lines of novel specific ionic liquids based imidazole, benzothiazole conjugates. *Int. J. Mol. Sci.* **2019**, *20*, 2865−2885.
(28) Wani, W. A.; Al-Othman, Z.; Ali, I.; Saleem, K.; Hsieh, M. F. Copper (II), nickel (II), and ruthenium (III) complexes of an oxopyrrolidine-based heterocyclic ligand as anticancer agents. *J. Coord. Chem.* **2014**, *67*, 2110−2130.
(29) Ali, I.; Wani, W. A.; Saleem, K.; Hsieh, M.-F. Anticancer metallodrugs of glutamic acid sulphonamides: *in silico*, DNA binding, hemolysis and anticancer studies. *RSC Adv.* **2014**, *4*, 29629−29641.
(30) Ali, I.; Wani, W. A.; Saleem, K.; Hseih, M.-F. Design and synthesis of thalidomide based dithiocarbamate Cu (II), Ni (II) and Ru (III) complexes as anticancer agents. *Polyhedron* **2013**, *56*, 134−143.
(31) Ali, I.; Haque, A.; Saleem, K.; Hsieh, M.-F. Curcumin-I Knoevenagel's condensates and their Schiff's bases as anticancer agents: Synthesis, pharmacological and simulation studies. *Bioorg. Med. Chem.* **2013**, *21*, 3808−3820.
(32) (a) Shahabadi, N.; Kashanian, S.; Mahdavi, M.; Sourinejad, N. DNA interaction and DNA cleavage studies of a new platinum (II) complex containing aliphatic and aromatic dinitrogen ligands. *Bioinorg. Chem. Appl.* **2011**, *2011*, No. 525794. (b) Roviello, G. N.; Vicidomini, C.; Di Gaetano, S.; Capasso, D.; Musumeci, D.; Roviello, V. Solid phase synthesis and RNA-binding activity of an arginine-containing nucleopeptide. *RSC Adv.* **2016**, *6*, 14140−14148. (c) Roviello, G. N.; Musumeci, D.; Moccia, M.; Castiglione, M.; Sapio, R.; Valente, M.; Bucci, E. M.; Perretta, G.; Pedone, C. *dab*Pna: Design, Synthesis, And Dna Binding Studies. *Nucleosides, Nucleotides Nucleic Acids* **2007**, *26*, 1307−1310.
(33) Erkkila, K. E.; Odom, D. T.; Barton, J. K. Recognition and reaction of metallo intercalators with DNA. *Chem. Rev.* **1999**, *99*, 2777−2796.
(34) Chen, L. M.; Liu, J.; Chen, J. C.; Tan, C. P.; Shi, S.; Zheng, K.-C.; Ji, L. N. Synthesis, characterization, DNA-binding and spectral properties of complexes [Ru (L) 4 (dppz)] 2+(L = Im and MeIm). *J. Inorg. Biochem.* **2008**, *102*, 330−341.
(35) Pasternack, R. F.; Gibbs, E. J.; Villafranca, J. J. Interactions of porphyrins with nucleic acids. *Biochemistry* **1983**, *22*, 5409−5417.
(36) Zhao, P.; Xu, L. C.; Huang, J. W.; Liu, J.; Yu, H. C.; Zheng, K. C.; Ji, L. N. Experimental and DFT studies on DNA binding and photocleavage of two cationic porphyrins: effects of the introduction of a carboxyphenyl into pyridinium porphyrin. *Spectrochim. Acta, Part A* **2008**, *71*, 1216−1223.
(37) Arjmand, F.; Aziz, M.; Chauhan, M. Synthesis, spectroscopic studies of new water-soluble Co (II) and Cu (II) macrocyclic complexes of 4, 15-bis (2-hydroxyethyl)-2, 4, 6, 13, 15, 17-hexaazatricyclodocosane: their interaction studies with calf thymus DNA and guanosine 5′ monophosphate. *J. Inclusion Phenom. Macrocyclic Chem.* **2008**, *61*, 265−278.
(38) Sun, Y.; Zhang, H.; Bi, S.; Zhou, X.; Wang, L.; Yan, Y. Studies on the arctiin and its interaction with DNA by spectral methods. *J. Lumin.* **2011**, *131*, 2299−2306.
(39) Küng, A.; Pieper, T.; Wissiack, R.; Rosenberg, E.; Keppler, B. K. Hydrolysis of the tumor-inhibiting ruthenium (III) complexes HIm trans[$RuCl_4(im)_2$] and HInd trans-[RuCl4 (ind) 2] investigated by means of HPCE and HPLC-MS. *JBIC, J. Biol. Inorg. Chem.* **2001**, *6*, 292−299.
(40) Bacac, M.; Hotze, A. C.; Van Der Schilden, K.; Haasnoot, J. G.; Pacor, S.; Alessio, E.; Sava, G.; Reedijk, J. The hydrolysis of the anti-cancer ruthenium complex NAMI-A affects its DNA binding and antimetastatic activity: an NMR evaluation. *J. Inorg. Biochem.* **2004**, *98*, 402−412.
(41) Lipinski, C. A.; Lombardo, F.; Dominy, B. W.; Feeney, P. J. Experimental and computational approaches to estimate solubility and permeability in drug discovery and development settings. *Adv. Drug Delivery Rev.* **2012**, *64*, 4−17.
(42) Kang, S.; Zeng, H.; Li, H.; Wang, H. 2-Chloro-N-(4-fluoro-phen-yl)acetamide. *Acta Crystallogr., Sect. E: Struct. Rep. Online* **2008**, *64*, No. o1194.
(43) Tanja, M. W.; Frederik, D.; Christoph, G.; Herwig, H.; Inge, L.; Karen, R.; Andreas, J. S.; Arnold, E. S.; Chris, A. T.; Stephen, G. W.; Heidrun, W. Probing the aglycon binding site of a β-glucosidase: a collection of C-1-modified 2,5-dideoxy-2,5-imino-d-mannitol derivatives and their structure-activity relationships as competitive inhibitors. *Bioorg. Med. Chem.* **2009**, *19*, 4643.
(44) Wolfe, A.; Shimer, G. H., Jr.; Meehan, T. Polycyclic aromatic hydrocarbons physically intercalate into duplex regions of denatured DNA. *Biochemistry* **1987**, *26*, 6392−6396.
(45) Martin, A.; Clynes, M. Comparison of 5 microplate colorimetric assays for in vitro cytotoxicity testing and cell proliferation assays. *Cytotechnology* **1993**, *11*, 49−58.
(46) Sanner, M. F. Python: A programming language for software integration and development. *J. Mol. Graphics Modell.* **1999**, *17*, 57−61.
(47) Huey, R.; Morris, G. M.; Olson, A. J.; Goodsell, D. S. A semiempirical free energy force field with charge-based desolvation. *J. Comput. Chem.* **2007**, 1145−1152.

https://dx.doi.org/10.1021/acsomega.9b03468
ACS Omega 2020, 5, 4807−4815